



PERGAMON

Journal of Quantitative Spectroscopy &
Radiative Transfer 83 (2004) 599–618

Journal of
Quantitative
Spectroscopy &
Radiative
Transfer

www.elsevier.com/locate/jqsrt

High-resolution spectrum of the $v_1 + v_4(E)$, $v_3 + v_4(E)$, $v_3 + v_4(A_1)$, and $v_3 + v_4(A_2)$ bands of the PH₃ molecule: assignments and preliminary analysis

O.N. Ulenikov^{a,*}, E.S. Bekhtereva^a, V.A. Kozinskaia^a, Jing-Jing Zheng^b,
Sheng-Gui He^b, Shui-Ming Hu^b, Qing-Shi Zhu^b, C. Leroy^c, L. Pluchart^c

^aLaboratory of Molecular Spectroscopy, Physics Department, Tomsk State University, Lenin Avenue 36,
Tomsk 634050, Russia, and Institute of Atmospheric Optics SB RAN, Tomsk 634055, Russia

^bOpen Laboratory of Bond Selective Chemistry, University of Science and Technology of China,
Hefei 230026, China

^cLaboratoire de physique, UMR CNRS 5027, Université de Bourgogne, 9 Avenue A. Savary, B.P. 47 870,
F-21078 Dijon, France

Received 19 September 2002; accepted 27 February 2003

Abstract

The high-resolution (0.005 cm^{-1}) Fourier transform infrared spectrum of PH₃ is recorded in the region between 3280 and 3580 cm^{-1} where the following bands are located: $v_1 + v_4(E)$, $v_3 + v_4(E)$, $v_3 + v_4(A_1)$, forbidden on symmetry band $v_3 + v_4(A_2)$, and very weak bands $v_1 + v_2(A_1)$, $v_2 + v_3(E)$. Transitions are assigned to the first four ones. Vibrational analysis of known experimental data is made.

© 2003 Elsevier Ltd. All rights reserved.

Keywords: Vibrational–rotational spectra; PH₃ molecule

1. Introduction

The high-resolution infrared spectra of phosphine can be used as an important source of information for several purposes, such as atmospheric studies of Earth and giant planets, investigation of industrial pollution, and for studies on the fundamental properties of pyramid type molecules. As a consequence, phosphine has been the subject of numerous studies of high resolution both pure

* Corresponding author.

E-mail address: ulenikov@phys.tsu.ru (O.N. Ulenikov).

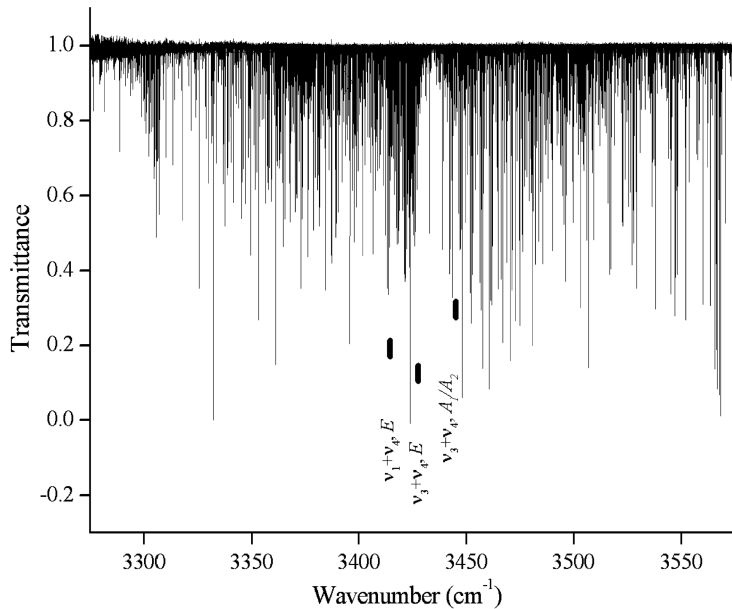


Fig. 1. An overview of the infrared spectrum from 3280 to 3580 cm^{-1} of PH_3 is shown. The vibrational band centers are approximately indicated. Experimental conditions: absorption path length 15 m, pressure 40 Pa, instrumental resolution 0.005 cm^{-1} , room temperature.

rotational and vibration–rotational spectra. However, most of the earlier studies have been devoted to the ground vibrational state, the deformational fundamentals ν_2 and ν_4 and their overtones, ν_1 and ν_3 stretching fundamentals, see, e.g., Ref. [1], references therein, and also Ref. [2]. To date, there were no high-resolution analysis of combination bands which correspond simultaneous excitations of the stretching and deformational vibrations. At the same time, high-resolution studies of such type bands can give information about the strength of connections between stretching and deformational motions in a molecule. In its turn, the last circumstance is important to understand the mechanisms of formation and/or destruction of the local mode behavior of the PH_3 molecule.

In this study, we present the assignment and preliminary analysis of the strongest of such type combination bands, $\nu_1 + \nu_4$ and $\nu_3 + \nu_4$, which are located in the region of 3280–3580 cm^{-1} and which were recorded for the first time with a high resolution (an overview of the spectrum is shown in Fig. 1). Besides the above-mentioned pure fundamental interest, the study of the $\nu_1 + \nu_4$ and $\nu_3 + \nu_4$ bands has an additional importance from an applied point of view. Since these bands are strong enough and located in a region of practically total absence of water absorption (water lines are presented in the shortwave part of the region only), they can be used to monitor the PH_3 . As a consequence, the results of the present contribution can be considered as an important addition to the modern data bases.

Since the $\nu_3 + \nu_4$ band consists of three subbands, $\nu_3 + \nu_4(E)$, $\nu_3 + \nu_4(A_1)$, and $\nu_3 + \nu_4(A_2)$, experimentally recorded high-resolution spectrum is a very complicated mixture of four totally overlapped and strongly interacting bands, which show very unusual dependence of the wave numbers of trans-

sitions on quantum numbers J and K . As a consequence, a correct and unambiguous mathematical description of the spectrum is needed in additional correct information on the fundamental parameters of the PH_3 molecule. Namely, correct numerical estimations of the values of band centers and of the main resonance interaction parameters are needed. That can be made, for example, on the basis of knowledge of an intramolecular potential function. Unfortunately, as the analysis shows, such information known in the modern spectroscopic literature (see, e.g., [3]), is not completely correct. For this reason, we limit our present consideration to preliminary analysis of the spectrum and assignments of transitions.

2. Experimental details

The PH_3 sample was purchased from Nanjing Special Gas Company with the stated purity of 99.9%. The spectrum was recorded at room temperature with a Bruker IFS 120HR Fourier-transform interferometer (Hefei, China), which is equipped with a path length adjustable multi-pass gas cell. The spectrum was recorded at room temperature with a sample pressure of 40 Pa and absorption path length of 15 m. A tungsten source, a CaF_2 beamsplitter, two optical band pass filters whose cutoff frequencies were 3150–4350 and 3310–2500 cm^{-1} and a liquid-nitrogen cooled InSb detector were used. The unapodized resolution was 0.005 cm^{-1} . The lines of H_2O were used to calibrate the position of the PH_3 lines by comparison with those listed in the GEISA 97 database. The accuracy of the not-very-weak unblended and nonsaturated lines was estimated to be no worse than 0.0004–0.0005 cm^{-1} . The overview spectrum and two small parts of the recorded high resolution spectrum are presented in Figs. 2 and 3, for illustration.

3. Description of the spectrum and assignments of transition

As is seen from Fig. 1, all four bands, $v_1 + v_4(E)$, $v_3 + v_4(E)$, $v_3 + v_4(A_1)$, and $v_3 + v_4(A_2)$, are located very closely and overlap each other. Because of strong resonance interactions, all the allowed interactions on symmetry bands, $v_1 + v_4(E)$, $v_3 + v_4(E)$, and $v_3 + v_4(A_1)$ have comparable strengths. Moreover, the presence of resonance interactions leads to appearance of sets of transitions belonging to the forbidden interaction on symmetry $v_3 + v_4(A_2)$ band (some such transitions, marked by open circles, can be seen in Figs. 2 and 3). At the high frequency region, lines belonging to the water vapor can be seen. However, an overlapping of the PH_3 and H_2O bands is weak. In the long wave part of the analyzed spectrum, the bands $v_1 + v_2$ and $v_2 + v_3$ are located. However, these two bands are considerably weaker than the ones considered in the present study, and only a few of the transitions belonging to the $v_1 + v_2$ and $v_2 + v_3$ bands can be seen in the recorded spectrum.

The assignment of transitions was fulfilled on the basis of the Ground State Combination Differences method, and the ground state energies were calculated with the parameters from Ref. [1]. As a result of assignment, sets of transitions of the type $(J' K' \Gamma') \leftarrow (J K \Gamma)$ (with fixed values of the quantum numbers K , K' , symmetries Γ , Γ' , and different values of quantum numbers J , $J' = J, J \pm 1$) were found in the spectrum up to $K^{\max} = 13$ and $J^{\max} = 14$. At the same time, at that step of analysis, it was not possible to answer the question: to which concrete band does one or another concrete set of transitions $(J' K' \Gamma') \leftarrow (J K \Gamma)$ belong? Fortunately, two sets of the

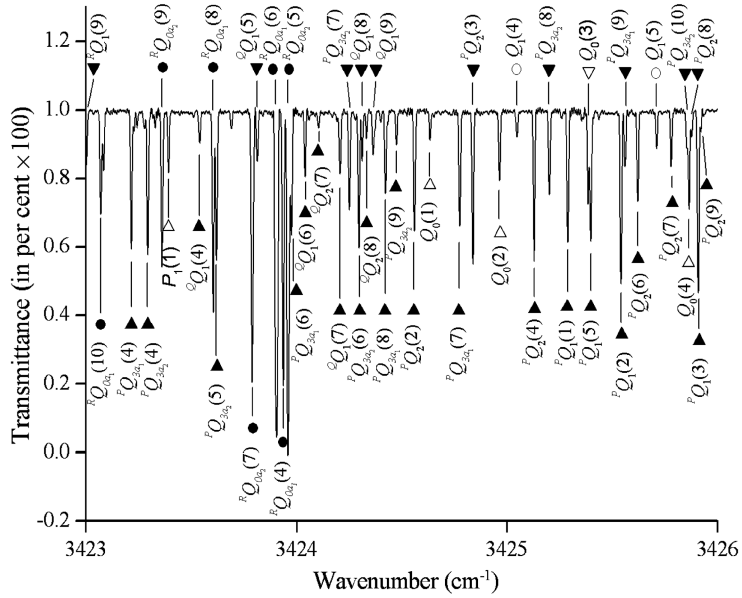


Fig. 2. A small portion of the spectrum in the region of the Q -branch of $v_1 + v_4$ band is illustrated. Transitions assigned to the $v_1 + v_4(E)$, $v_3 + v_4(E)$, $v_3 + v_4(A_1)$, and $v_3 + v_4(A_2)$ bands are marked by dark triangles, dark circles, open triangles, and open circles, respectively. Set of the $RQ_{K=0}(J)$ transitions of the $v_1 + v_4(E)$ band is seen on the left-hand side of the figure. Some transitions which belong to the “forbidden” band $v_3 + v_4(A_2)$ can also be seen.

$RQ_{K=0}(J)$ transitions, which undoubtedly indicate two doubly degenerated E -type bands ($v_1 + v_4(E)$ and $v_3 + v_4(E)$ in our case), can be found in the spectrum by way of simple visible inspection (one of them can be seen in Fig. 2). In its turn, the last circumstance allows one to make a conclusion that two E -type vibrational bands, $v_1 + v_4(E)$ and $v_3 + v_4(E)$, are located in a longer wave region, and the $v_3 + v_4(A_1)$ and $v_3 + v_4(A_2)$ bands are located in a shorter wave part (see Fig. 4). Finally, more than 90 per cent of experimentally recorded lines were assigned to the four studied bands, $v_1 + v_4(E)$, $v_3 + v_4(E)$, $v_3 + v_4(A_1)$, and $v_3 + v_4(A_2)$. The list of transitions is presented in Table 1. In this case, Columns 4 and 5 of that table give the experimental wave numbers of transitions and their transmittances, in cm^{-1} and per cent, respectively. The quantum numbers J' , K' and J , K of the upper and lower ro-vibrational states and their symmetries Γ' and Γ are presented in Columns 1 and 2, respectively. Column 3 shows the band to which the transition belongs.

Two interesting points should be specially mentioned here as the results of the assignments:

- (1) the presence of experimentally recorded numerous a_1/a_2 splittings for the states ($J K a_1, a_2$) with the value of quantum number $K = 1-10$, and
- (2) the appearance of numerous and strong enough transitions belonging to the band $v_3 + v_4(A_2)$ which is forbidden on symmetry.

Both of these effects are caused by the presence of strong resonance interactions between all the four studied bands.

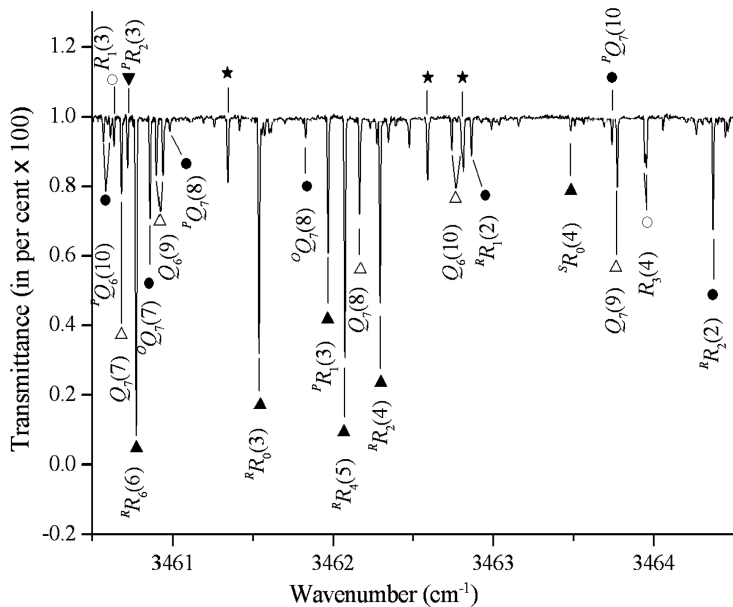


Fig. 3. A portion of the recorded spectrum in the region of the R -branch of the bands $v_1 + v_4$ and $v_3 + v_4$. Transitions assigned to the $v_1 + v_4(E)$, $v_3 + v_4(E)$, $v_3 + v_4(A_1)$, and $v_3 + v_4(A_2)$ bands are marked by dark triangles, dark circles, open triangles, and open circles, respectively. Three water vapor lines are marked by star. Some high K -value a_1/a_2 splittings can be seen.

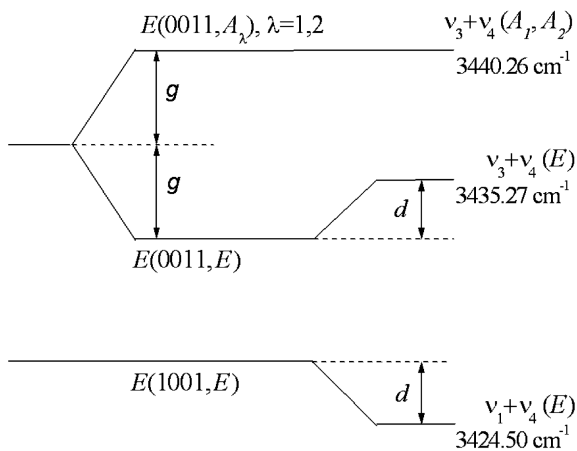


Fig. 4. Diagram of locations of some vibrational energy levels and interactions in the PH_3 molecule: g denotes splitting of the (0011) term into the E and A_1/A_2 components; d caused by the Fermi type resonance interaction between the $(1001, E)$ and $(0011, E)$ states.

Table 1 (continued)

Upper state <i>J' K' Γ'</i>	Lower state <i>J K Γ</i>	Band	Line position, exp., in cm ⁻¹	Trsm., in %	Upper state <i>J' K' Γ'</i>	Lower state <i>J K Γ</i>	Band	Line position, exp., in cm ⁻¹	Trsm., in %
6 5 a	7 6 a	$v_1 + v_4, E$	3353.2270	27.2	7 3 a ₂	8 0 a ₁	$v_3 + v_4, A_1$	3375.3826	84.4
7 2 a ₁	8 3 a ₂	$v_1 + v_4, E$	3353.2542	79.0	7 2 a ₁	8 3 a ₂	$v_3 + v_4, E$	3375.6008	90.2
7 2 a ₂	8 3 a ₁	$v_1 + v_4, E$	3353.7807	78.2	7 1 e	8 1 e	$v_3 + v_4, A_1$	3375.7918	85.6
6 4 e	7 4 e	$v_3 + v_4, A_2$	3354.1497	86.9	4 3 e	5 4 e	$v_1 + v_4, E$	3376.1131	43.6
7 1 e	8 2 e	$v_1 + v_4, E$	3354.7976	84.1	6 3 e	7 2 e	$v_3 + v_4, E$	3376.5868	84.7
9 4 e	10 1 e	$v_3 + v_4, E$	3354.8647	96.8	8 5 e	9 5 e	$v_3 + v_4, A_1$	3376.7927	94.9
10 2 e	11 1 e	$v_3 + v_4, A_1$	3355.1796	93.6	7 2 e	8 2 e	$v_3 + v_4, A_1$	3377.0378	85.8
9 3 e	10 2 e	$v_3 + v_4, E$	3355.8180	93.2	4 2 e	5 1 e	$v_1 + v_4, E$	3377.1008	89.5
7 1 e	8 1 e	$v_3 + v_4, A_2$	3355.9218	96.8	4 1 a ₁	5 0 a ₂	$v_1 + v_4, E$	3377.4350	95.5
6 3 e	7 2 e	$v_1 + v_4, E$	3356.0706	94.2	5 1 a ₁	6 3 a ₂	$v_3 + v_4, E$	3377.7863	90.0
10 1 e	11 2 e	$v_3 + v_4, A_1$	3356.2197	93.9	6 4 e	7 1 e	$v_3 + v_4, E$	3377.7863	90.0
9 6 e	10 4 e	$v_3 + v_4, E$	3356.3657	96.6	8 5 a ₂	9 6 a ₁	$v_3 + v_4, E$	3378.1703	89.0
6 4 e	7 5 e	$v_1 + v_4, E$	3356.5421	58.0	8 5 a ₁	9 6 a ₂	$v_3 + v_4, E$	3378.3083	92.3
9 4 a ₁	10 3 a ₂	$v_3 + v_4, E$	3356.6632	93.3	7 3 e	8 4 e	$v_3 + v_4, E$	3378.4934	77.2
9 4 a ₂	10 3 a ₁	$v_3 + v_4, E$	3356.7648	87.0	6 4 a ₁	7 3 a ₂	$v_3 + v_4, E$	3378.6900	92.4
7 0 e	8 1 e	$v_1 + v_4, E$	3357.1351	77.2	4 2 a ₂	5 3 a ₁	$v_1 + v_4, E$	3378.7423	50.9
9 5 e	10 4 e	$v_3 + v_4, E$	3357.1778	95.6	4 2 a ₁	5 3 a ₂	$v_1 + v_4, E$	3378.8201	51.0
7 1 a ₂	8 0 a ₁	$v_3 + v_4, E$	3357.2552	67.9	7 0 a ₂	8 3 a ₁	$v_3 + v_4, A_1$	3378.8893	83.0
8 2 e	9 1 e	$v_3 + v_4, E$	3357.2767	94.9	7 3 a ₁	8 3 a ₂	$v_3 + v_4, A_1$	3379.2139	88.9
7 1 e	8 2 e	$v_3 + v_4, A_2$	3357.4851	94.1	6 5 a ₁	7 3 a ₂	$v_3 + v_4, E$	3379.3632	95.2
10 0 a ₁	11 3 a ₂	$v_3 + v_4, A_1$	3357.6586	92.5	6 5 a ₂	7 3 a ₁	$v_3 + v_4, E$	3379.4123	96.7
8 6 a ₁	9 6 a ₂	$v_3 + v_4, A_1$	3379.4975	96.8	9 5 a ₂	9 3 a ₁	$v_1 + v_4, E$	3403.1848	97.2
8 6 a ₂	9 6 a ₁	$v_3 + v_4, A_1$	3379.5206	96.7	8 5 e	8 2 e	$v_1 + v_4, E$	3403.8708	96.2
9 8 a	10 9 a	$v_3 + v_4, E$	3379.5646	64.9	7 6 e	7 5 e	$v_1 + v_4, E$	3404.1355	75.6
11 11 e	11 10 e	$v_1 + v_4, E$	3379.6444	96.8	8 6 e	8 5 e	$v_1 + v_4, E$	3404.9757	75.4
6 5 e	7 4 e	$v_3 + v_4, E$	3379.9775	93.9	4 4 e	5 4 e	$v_3 + v_4, A_1$	3405.2807	92.4
4 1 e	5 1 e	$v_3 + v_4, A_2$	3380.5875	98.3	3 0 a ₂	4 0 a ₁	$v_3 + v_4, A_1$	3405.5964	66.2
4 1 e	5 2 e	$v_1 + v_4, E$	3380.6652	61.2	9 6 e	9 5 e	$v_1 + v_4, E$	3405.7322	78.3
8 6 e	9 7 e	$v_3 + v_4, E$	3381.0689	75.8	1 1 a ₂	2 0 a ₁	$v_3 + v_4, E$	3406.3369	73.4
4 1 a ₁	5 0 a ₂	$v_3 + v_4, E$	3381.4943	52.0	3 1 e	4 1 e	$v_3 + v_4, A_1$	3406.3724	73.6
7 4 e	8 4 e	$v_3 + v_4, A_1$	3381.5622	83.8	10 6 e	10 5 e	$v_1 + v_4, E$	3406.4004	83.1
6 0 a ₁	7 0 a ₂	$v_3 + v_4, A_1$	3381.7253	96.2	4 4 e	5 5 e	$v_3 + v_4, E$	3406.4694	82.3
4 0 e	5 1 e	$v_1 + v_4, E$	3381.9221	56.7	1 1 e	2 2 e	$v_1 + v_4, E$	3406.5274	43.9
4 1 e	5 2 e	$v_3 + v_4, A_2$	3382.1762	90.5	9 8 a	9 9 a	$v_1 + v_4, E$	3406.6517	88.8
6 3 a ₁	7 0 a ₂	$v_3 + v_4, A_1$	3382.6184	83.0	5 4 e	5 2 e	$v_1 + v_4, E$	3406.9332	97.8
3 3 a	4 3 a	$v_3 + v_4, A_2$	3382.6908	86.1	11 6 e	11 5 e	$v_1 + v_4, E$	3407.0769	87.3
7 4 e	8 5 e	$v_3 + v_4, E$	3382.7868	92.1	3 2 a ₂	4 3 a ₁	$v_3 + v_4, E$	3407.3175	77.7
6 1 e	7 1 e	$v_3 + v_4, A_1$	3382.8408	94.9	1 0 e	2 1 e	$v_1 + v_4, E$	3407.4850	61.3
5 2 e	6 1 e	$v_3 + v_4, E$	3383.0063	91.6	3 2 a ₁	4 3 a ₂	$v_3 + v_4, E$	3407.6002	74.1
6 2 a ₂	7 3 a ₁	$v_3 + v_4, E$	3383.2361	86.0	10 8 a	10 9 a	$v_1 + v_4, E$	3407.7041	87.3
5 3 e	6 1 e	$v_3 + v_4, E$	3383.6020	95.6	5 5 e	5 4 e	$v_1 + v_4, E$	3408.0012	74.1
10 10 a ₂	10 9 a ₁	$v_1 + v_4, E$	3384.2088	90.4	7 4 e	7 2 e	$v_1 + v_4, E$	3408.2996	96.7
7 5 e	8 5 e	$v_3 + v_4, A_1$	3384.2842	94.6	3 2 e	4 2 e	$v_3 + v_4, A_1$	3408.3316	80.3
8 7 e	9 8 e	$v_3 + v_4, E$	3384.3880	84.9	6 5 e	6 4 e	$v_1 + v_4, E$	3408.7256	66.5
6 1 e	7 2 e	$v_3 + v_4, A_1$	3384.4142	84.3	2 2 e	3 1 e	$v_3 + v_4, E$	3409.3240	94.9
3 3 e	4 4 e	$v_1 + v_4, E$	3384.4958	34.5	7 5 e	7 4 e	$v_1 + v_4, E$	3409.4319	67.4
6 2 e	7 2 e	$v_3 + v_4, A_1$	3384.6484	96.0	8 7 e	8 8 e	$v_1 + v_4, E$	3409.6817	92.3

Table 1 (continued)

Upper state <i>J' K' Γ'</i>	Lower state <i>J K Γ</i>	Band	Line position, exp., in cm ⁻¹	Trsm., in %	Upper state <i>J' K' Γ'</i>	Lower state <i>J K Γ</i>	Band	Line position, exp., in cm ⁻¹	Trsm., in %
5 3 e	6 4 e	$v_3 + v_4, E$	3394.6273	74.8	3 3 a	3 3 a	$v_3 + v_4, A_2$	3418.2892	80.4
5 3 a ₂	6 3 a ₁	$v_3 + v_4, A_1$	3394.8511	97.4	9 4 e	9 4 e	$v_3 + v_4, A_2$	3418.4142	94.0
9 8 e	9 7 e	$v_1 + v_4, E$	3395.0143	81.2	4 2 a ₂	4 0 a ₁	$v_1 + v_4, E$	3418.4354	95.3
4 4 e	5 2 e	$v_3 + v_4, E$	3395.2903	95.9	7 3 e	7 2 e	$v_1 + v_4, E$	3418.5594	50.7
2 2 a	3 3 a	$v_1 + v_4, E$	3395.7466	20.2	11 3 e	11 2 e	$v_1 + v_4, E$	3418.7099	84.5
8 6 e	8 4 e	$v_1 + v_4, E$	3395.9233	98.3	6 4 e	6 5 e	$v_1 + v_4, E$	3418.7565	71.5
2 1 e	3 1 e	$v_1 + v_4, E$	3396.2573	85.7	8 3 e	8 2 e	$v_1 + v_4, E$	3418.7691	56.0
10 8 e	10 7 e	$v_1 + v_4, E$	3396.2573	85.7	10 3 e	10 2 e	$v_1 + v_4, E$	3418.8294	71.0
5 3 e	6 5 e	$v_3 + v_4, E$	3396.3194	97.4	9 3 e	9 2 e	$v_1 + v_4, E$	3418.8471	63.8
6 6 e	7 7 e	$v_3 + v_4, E$	3396.9390	60.8	6 2 a ₂	6 0 a ₁	$v_1 + v_4, E$	3419.2277	88.2
12 11 a	12 12 a	$v_1 + v_4, E$	3396.9619	96.4	7 4 e	7 5 e	$v_1 + v_4, E$	3419.3858	71.8
5 4 e	6 4 e	$v_3 + v_4, A_1$	3397.1573	89.8	9 2 a ₁	9 0 a ₂	$v_1 + v_4, E$	3419.7990	79.7
4 0 a ₁	5 0 a ₂	$v_3 + v_4, A_1$	3397.4673	79.2	8 4 e	8 5 e	$v_1 + v_4, E$	3420.0042	75.3
6 5 e	7 7 e	$v_3 + v_4, E$	3397.5643	95.9	6 3 a ₂	6 3 a ₁	$v_3 + v_4, A_2$	3420.0376	95.4
11 8 e	11 7 e	$v_1 + v_4, E$	3397.6066	90.5	6 3 a ₁	6 3 a ₂	$v_3 + v_4, A_2$	3420.0685	94.9
2 1 e	3 2 e	$v_1 + v_4, E$	3397.8567	47.0	7 3 a ₁	7 3 a ₂	$v_3 + v_4, A_2$	3420.5768	91.4
2 1 a ₁	3 0 a ₂	$v_3 + v_4, E$	3397.8833	58.4	4 3 e	4 4 e	$v_1 + v_4, E$	3420.5993	75.3
4 3 a ₁	5 0 a ₂	$v_3 + v_4, A_1$	3397.9171	91.0	4 2 e	4 1 e	$v_3 + v_4, A_2$	3420.6601	96.3
4 1 e	5 1 e	$v_3 + v_4, A_1$	3398.2619	76.2	8 3 a ₂	8 3 a ₁	$v_3 + v_4, A_2$	3420.8132	80.8
5 4 e	6 5 e	$v_3 + v_4, E$	3398.3743	76.3	2 2 e	2 1 e	$v_1 + v_4, E$	3420.9384	59.6
7 7 a	7 6 a	$v_1 + v_4, E$	3398.5345	73.1	9 3 a ₁	9 3 a ₂	$v_3 + v_4, A_2$	3420.9546	87.2
4 2 a ₁	5 3 a ₂	$v_3 + v_4, E$	3398.5800	84.8	8 3 a ₁	8 3 a ₂	$v_3 + v_4, A_2$	3420.9684	80.7
2 0 e	3 1 e	$v_1 + v_4, E$	3398.8407	56.8	5 2 e	5 2 e	$v_3 + v_4, A_2$	3421.1191	89.0
4 2 a ₂	5 3 a ₁	$v_3 + v_4, E$	3399.2532	77.2	5 3 e	5 4 e	$v_1 + v_4, E$	3421.1349	65.5
8 7 a	8 6 a	$v_1 + v_4, E$	3399.5898	66.6	3 2 e	3 1 e	$v_1 + v_4, E$	3421.2396	38.8
4 1 e	5 2 e	$v_3 + v_4, A_1$	3399.8486	94.8	9 4 e	9 5 e	$v_1 + v_4, E$	3421.4747	91.6
5 5 e	6 5 e	$v_3 + v_4, A_1$	3399.9277	96.1	4 2 e	4 1 e	$v_1 + v_4, E$	3421.5610	36.7
4 2 e	5 2 e	$v_3 + v_4, A_1$	3400.1311	81.7	6 3 e	6 4 e	$v_1 + v_4, E$	3421.6695	65.9
11 10 e	11 11 e	$v_1 + v_4, E$	3400.2023	97.3	5 2 e	5 1 e	$v_1 + v_4, E$	3421.8799	37.5
9 7 a ₁	9 6 a ₂	$v_1 + v_4, E$	3400.5246	85.9	7 3 e	7 4 e	$v_1 + v_4, E$	3422.1671	68.4
3 2 e	4 1 e	$v_3 + v_4, E$	3400.5768	92.1	6 2 e	6 1 e	$v_1 + v_4, E$	3422.2095	45.7
9 7 a ₂	9 6 a ₁	$v_1 + v_4, E$	3400.6238	84.8	7 2 e	7 1 e	$v_1 + v_4, E$	3422.5310	57.7
10 7 a	10 6 a	$v_1 + v_4, E$	3401.5194	73.4	1 0 a ₂	2 0 a ₁	$v_3 + v_4, A_1$	3422.5700	75.7
1 1 a ₂	2 0 a ₁	$v_1 + v_4, E$	3401.8212	95.2	8 3 e	8 4 e	$v_1 + v_4, E$	3422.6017	74.4
5 5 a	6 6 a	$v_3 + v_4, E$	3401.8468	43.8	5 2 e	5 2 e	$v_3 + v_4, A_2$	3422.7055	78.3
3 3 e	4 2 e	$v_3 + v_4, E$	3402.0752	93.4	1 1 e	1 1 e	$v_1 + v_4, E$	3422.7348	97.6
4 0 a ₁	5 3 a ₂	$v_3 + v_4, A_1$	3402.2328	85.7	8 2 e	8 1 e	$v_1 + v_4, E$	3422.7670	66.5
8 5 a ₂	8 3 a ₁	$v_1 + v_4, E$	3402.4777	97.0	11 1 a ₁	11 0 a ₂	$v_1 + v_4, E$	3422.7760	80.3
11 7 a	11 6 a	$v_1 + v_4, E$	3402.5037	88.6	3 2 a ₁	3 3 a ₂	$v_1 + v_4, E$	3422.8131	60.6
4 3 a ₂	5 3 a ₁	$v_3 + v_4, A_1$	3402.5891	85.8	3 2 a ₂	3 3 a ₁	$v_1 + v_4, E$	3422.8382	69.2
4 3 a ₁	5 3 a ₂	$v_3 + v_4, A_1$	3402.6818	91.8	9 3 e	9 4 e	$v_1 + v_4, E$	3422.9718	71.7
4 3 e	5 4 e	$v_3 + v_4, E$	3402.8411	67.8	9 2 e	9 1 e	$v_1 + v_4, E$	3423.0032	84.1
9 5 a ₁	9 3 a ₂	$v_1 + v_4, E$	3403.0969	96.8	6 2 e	6 2 e	$v_3 + v_4, A_2$	3423.0032	84.1
6 6 e	6 5 e	$v_1 + v_4, E$	3403.1566	83.8	10 1 a ₂	10 0 a ₁	$v_1 + v_4, E$	3423.0717	69.6
4 2 a ₂	4 3 a ₁	$v_1 + v_4, E$	3423.2162	59.4	5 4 e	5 2 e	$v_3 + v_4, E$	3440.5628	92.5
4 2 a ₁	4 3 a ₂	$v_1 + v_4, E$	3423.2938	58.1	6 4 a ₂	6 3 a ₁	$v_3 + v_4, E$	3440.7579	92.4
9 1 a ₁	9 0 a ₂	$v_1 + v_4, E$	3423.3596	54.2	5 5 a	5 3 a	$v_3 + v_4, E$	3440.8040	96.5

Table 1 (continued)

Upper state <i>J' K' Γ'</i>	Lower state <i>J K Γ</i>	Band	Line position, exp., in cm ⁻¹	Trsm., in %	Upper state <i>J' K' Γ'</i>	Lower state <i>J K Γ</i>	Band	Line position, exp., in cm ⁻¹	Trsm., in %
1 1 e	2 1 e	$v_3 + v_4, A_1$	3423.3906	81.7	6 4 a ₁	6 3 a ₂	$v_3 + v_4, E$	3440.8663	90.2
4 1 e	4 1 e	$v_1 + v_4, E$	3423.5389	90.4	6 3 e	6 1 e	$v_3 + v_4, E$	3440.9320	97.7
3 1 a ₁	3 0 a ₂	$v_1 + v_4, E$	3423.6036	40.3	7 4 e	7 1 e	$v_3 + v_4, E$	3441.1663	97.7
8 1 a ₂	8 0 a ₁	$v_1 + v_4, E$	3423.6036	40.3	1 1 e	1 1 e	$v_3 + v_4, A_1$	3441.1969	79.6
5 2 a ₁	5 3 a ₂	$v_1 + v_4, E$	3423.6190	56.1	5 5 e	5 4 e	$v_3 + v_4, E$	3441.3119	84.4
4 1 a ₂	4 0 a ₁	$v_1 + v_4, E$	3423.7884	20.2	2 1 e	2 1 e	$v_3 + v_4, A_1$	3441.4699	88.8
7 1 a ₁	7 0 a ₂	$v_1 + v_4, E$	3423.7884	20.2	6 4 e	6 2 e	$v_3 + v_4, E$	3441.5245	91.6
5 1 e	5 1 e	$v_1 + v_4, E$	3423.8132	85.0	7 4 a ₂	7 3 a ₁	$v_3 + v_4, E$	3441.8933	93.7
6 1 a ₂	6 0 a ₁	$v_1 + v_4, E$	3423.9048	43.0	3 1 e	3 1 e	$v_3 + v_4, A_1$	3441.9588	90.3
5 1 a ₁	5 0 a ₂	$v_1 + v_4, E$	3423.9597	0.90	6 5 e	6 4 e	$v_3 + v_4, E$	3442.1720	80.3
6 2 a ₂	6 3 a ₁	$v_1 + v_4, E$	3423.9757	63.6	2 1 a ₁	1 0 a ₂	$v_3 + v_4, E$	3442.3892	39.0
6 1 e	6 1 e	$v_1 + v_4, E$	3424.0407	80.6	7 5 a ₂	7 3 a ₁	$v_3 + v_4, E$	3442.5930	95.6
7 2 e	7 2 e	$v_1 + v_4, E$	3424.1054	94.8	8 3 e	8 2 e	$v_3 + v_4, E$	3442.6810	97.3
7 1 e	7 1 e	$v_1 + v_4, E$	3424.2071	81.4	4 1 e	4 1 e	$v_3 + v_4, A_1$	3442.7221	95.1
7 2 a ₁	7 3 a ₂	$v_1 + v_4, E$	3424.2511	70.8	7 4 e	7 2 e	$v_3 + v_4, E$	3442.7402	95.0
6 2 a ₁	6 3 a ₂	$v_1 + v_4, E$	3424.2973	59.8	7 5 a ₁	7 3 a ₂	$v_3 + v_4, E$	3442.7983	87.9
8 1 e	8 1 e	$v_1 + v_4, E$	3424.3121	85.1	3 2 a ₂	3 3 a ₁	$v_3 + v_4, E$	3442.9153	92.5
8 2 e	8 2 e	$v_1 + v_4, E$	3424.3324	91.8	4 2 a ₁	4 3 a ₂	$v_3 + v_4, E$	3443.0544	88.9
9 1 e	9 1 e	$v_1 + v_4, E$	3424.3640	87.1	6 6 e	6 5 e	$v_3 + v_4, E$	3443.0763	87.1
8 2 a ₂	8 3 a ₁	$v_1 + v_4, E$	3424.4231	75.6	8 8 a	8 6 a	$v_3 + v_4, E$	3443.1307	85.8
9 2 a ₁	9 3 a ₂	$v_1 + v_4, E$	3424.4752	89.8	3 2 a ₁	3 3 a ₂	$v_3 + v_4, E$	3443.1990	88.6
2 1 e	2 2 e	$v_1 + v_4, E$	3424.5607	64.6	7 5 e	7 4 e	$v_3 + v_4, E$	3443.2753	92.5
1 1 a ₁	1 0 a ₂	$v_3 + v_4, E$	3424.6349	91.2	2 0 e	1 1 e	$v_1 + v_4, E$	3443.3478	83.0
7 2 a ₂	7 3 a ₁	$v_1 + v_4, E$	3424.7764	65.9	5 2 a ₂	5 3 a ₁	$v_3 + v_4, E$	3443.4429	90.3
3 1 e	3 2 e	$v_1 + v_4, E$	3424.8395	55.0	2 2 e	2 2 e	$v_3 + v_4, A_1$	3443.4781	63.9
2 1 a ₂	2 0 a ₁	$v_3 + v_4, E$	3424.9661	79.3	3 3 e	2 2 e	$v_1 + v_4, E$	3443.6526	32.6
4 1 e	4 1 e	$v_3 + v_4, A_2$	3425.0497	92.1	4 2 a ₂	4 3 a ₁	$v_3 + v_4, E$	3443.7275	88.1
4 1 e	4 2 e	$v_1 + v_4, E$	3425.1307	55.8	5 1 e	5 1 e	$v_3 + v_4, A_1$	3443.7531	94.8
8 2 a ₁	8 3 a ₂	$v_1 + v_4, E$	3425.2035	75.3	7 6 a ₁	7 3 a ₂	$v_3 + v_4, A_1$	3443.7742	94.2
1 0 e	1 1 e	$v_1 + v_4, E$	3425.2912	61.3	8 4 a ₂	8 3 a ₁	$v_3 + v_4, E$	3443.8039	96.4
3 1 a ₁	3 0 a ₂	$v_3 + v_4, E$	3425.3879	72.4	3 2 e	3 2 e	$v_3 + v_4, A_1$	3443.9227	75.9
5 1 e	5 2 e	$v_1 + v_4, E$	3425.4001	61.6	8 4 a ₁	8 3 a ₂	$v_3 + v_4, E$	3443.9401	92.2
2 0 e	2 1 e	$v_1 + v_4, E$	3425.5418	49.2	7 6 e	7 5 e	$v_3 + v_4, E$	3444.0213	84.5
9 2 a ₂	9 3 a ₁	$v_1 + v_4, E$	3425.5605	83.6	8 5 e	8 4 e	$v_3 + v_4, E$	3444.3355	90.5
6 1 e	6 2 e	$v_1 + v_4, E$	3425.6212	73.1	9 3 e	9 2 e	$v_3 + v_4, E$	3444.3630	98.5
5 1 e	5 1 e	$v_3 + v_4, A_2$	3425.7109	88.8	5 2 a ₁	5 3 a ₂	$v_3 + v_4, E$	3444.4576	84.2
7 1 e	7 2 e	$v_1 + v_4, E$	3425.7805	83.3	4 2 e	4 2 e	$v_3 + v_4, A_1$	3444.5965	81.2
10 2 a ₁	10 3 a ₂	$v_1 + v_4, E$	3425.8549	84.8	8 7 e	8 4 e	$v_3 + v_4, A_1$	3444.6704	98.4
4 1 a ₂	4 0 a ₁	$v_3 + v_4, E$	3425.8653	71.1	7 7 a	7 6 a	$v_3 + v_4, E$	3444.7510	80.2
8 1 e	8 2 e	$v_1 + v_4, E$	3425.8779	92.1	8 2 e	8 4 e	$v_3 + v_4, E$	3444.8979	94.3
3 0 e	3 1 e	$v_1 + v_4, E$	3425.9086	46.2	6 1 e	6 1 e	$v_3 + v_4, A_1$	3444.9982	94.9
9 1 e	9 2 e	$v_1 + v_4, E$	3425.9219	93.7	8 6 e	8 5 e	$v_3 + v_4, E$	3445.1561	78.4
5 1 a ₁	5 0 a ₂	$v_3 + v_4, E$	3426.3538	74.2	9 4 a ₁	9 3 a ₂	$v_3 + v_4, E$	3445.2238	95.3
4 0 e	4 1 e	$v_1 + v_4, E$	3426.3824	50.3	9 4 a ₂	9 3 a ₁	$v_3 + v_4, E$	3445.3236	94.4
4 1 e	4 2 e	$v_3 + v_4, A_2$	3426.6417	89.2	6 2 a ₂	6 3 a ₁	$v_3 + v_4, E$	3445.4121	83.5
6 1 a ₂	6 0 a ₁	$v_3 + v_4, E$	3426.8116	78.5	7 3 a ₁	7 0 a ₂	$v_3 + v_4, A_1$	3445.4834	95.6
7 1 e	7 1 e	$v_3 + v_4, A_2$	3426.8963	89.3	5 2 e	5 2 e	$v_3 + v_4, A_1$	3445.5498	86.7
5 0 e	5 1 e	$v_1 + v_4, E$	3426.9433	61.3	9 5 e	9 4 e	$v_3 + v_4, E$	3445.7615	93.2

Table 1 (continued)

Upper state <i>J' K' Γ'</i>	Lower state <i>J K Γ</i>	Band	Line position, exp., in cm ⁻¹	Trsm., in %	Upper state <i>J' K' Γ'</i>	Lower state <i>J K Γ</i>	Band	Line position, exp., in cm ⁻¹	Trsm., in %
7 1 e	6 1 e	$v_3 + v_4, A_1$	3508.9247	84.8	9 5 e	8 5 e	$v_3 + v_4, A_1$	3538.0091	86.5
9 1 e	8 2 e	$v_3 + v_4, A_2$	3508.9519	91.2	10 0 a ₁	9 0 a ₂	$v_3 + v_4, A_1$	3538.8397	87.1
9 4 a ₂	8 6 a ₁	$v_1 + v_4, E$	3509.0890	99.0	10 1 e	9 1 e	$v_3 + v_4, A_1$	3540.4885	93.5
7 1 a ₂	6 6 a ₁	$v_3 + v_4, E$	3509.5104	97.3	10 3 a ₁	9 0 a ₂	$v_3 + v_4, A_1$	3540.6297	94.4
8 2 e	7 2 e	$v_3 + v_4, E$	3509.5932	94.9	9 6 a ₂	8 6 a ₁	$v_3 + v_4, A_1$	3540.7749	88.8
9 3 e	8 5 e	$v_1 + v_4, E$	3509.6526	98.5	9 6 a ₁	8 6 a ₂	$v_3 + v_4, A_1$	3540.8117	88.4
10 2 a ₁	9 0 a ₂	$v_1 + v_4, E$	3509.7419	96.6	10 2 e	9 1 e	$v_3 + v_4, A_1$	3540.9844	94.2
7 2 e	6 2 e	$v_3 + v_4, A_1$	3510.1855	82.1	10 1 e	9 2 e	$v_3 + v_4, A_1$	3542.0453	92.7
8 4 a ₁	7 0 a ₂	$v_3 + v_4, E$	3510.2122	89.1	10 2 e	9 2 e	$v_3 + v_4, A_1$	3542.5413	92.9
7 0 a ₂	6 3 a ₁	$v_3 + v_4, A_1$	3512.0614	85.4	10 0 a ₁	9 3 a ₂	$v_3 + v_4, A_1$	3543.5160	94.6
7 3 a ₁	6 3 a ₂	$v_3 + v_4, A_1$	3512.3866	73.3	9 7 e	8 7 e	$v_3 + v_4, A_1$	3543.6886	93.1
8 4 e	7 1 e	$v_3 + v_4, E$	3512.8291	94.3	10 3 a ₂	9 3 a ₁	$v_3 + v_4, A_1$	3543.9392	87.4
7 3 a ₂	6 3 a ₁	$v_3 + v_4, A_1$	3513.2581	84.5	10 3 a ₁	9 3 a ₂	$v_3 + v_4, A_1$	3545.3056	90.4
9 1 a ₂	8 3 a ₁	$v_3 + v_4, E$	3513.5164	94.8	10 3 e	9 5 e	$v_3 + v_4, E$	3545.8033	96.8
8 3 e	7 2 e	$v_3 + v_4, E$	3513.6648	83.6	10 4 e	9 5 e	$v_3 + v_4, E$	3546.1987	97.7
8 2 a ₁	7 3 a ₂	$v_3 + v_4, E$	3514.1990	86.2	11 9 e	10 8 e	$v_3 + v_4, E$	3547.9144	61.0
10 2 a ₁	9 3 a ₂	$v_1 + v_4, E$	3514.4177	87.8	11 8 e	10 7 e	$v_3 + v_4, E$	3548.0070	78.9
10 1 e	9 2 e	$v_1 + v_4, E$	3514.4644	89.2	11 7 a ₂	10 6 a ₁	$v_3 + v_4, E$	3548.0608	88.1
7 4 e	6 4 e	$v_3 + v_4, A_1$	3514.7707	78.7	11 7 a ₁	10 6 a ₂	$v_3 + v_4, E$	3548.0866	87.1
8 4 a ₂	7 3 a ₁	$v_3 + v_4, E$	3514.7999	86.4	11 10 a	10 9 a	$v_3 + v_4, E$	3548.1097	38.9
8 4 a ₁	7 3 a ₂	$v_3 + v_4, E$	3514.9384	87.6	11 6 a ₂	10 3 a ₁	$v_3 + v_4, A_1$	3548.3478	94.7
8 5 e	7 4 e	$v_3 + v_4, E$	3515.3487	76.7	11 6 a ₁	10 3 a ₂	$v_3 + v_4, A_1$	3548.4503	94.6
8 7 e	7 4 e	$v_3 + v_4, A_1$	3515.6852	90.8	10 5 e	9 5 e	$v_3 + v_4, A_1$	3548.5944	90.1
8 2 e	7 4 e	$v_3 + v_4, E$	3515.9128	98.4	10 5 a ₁	9 6 a ₂	$v_3 + v_4, E$	3549.2650	95.9
11 3 e	10 2 e	$v_1 + v_4, E$	3515.9915	95.8	11 0 a ₂	10 0 a ₁	$v_3 + v_4, A_1$	3549.7808	88.1
8 6 a ₁	7 3 a ₂	$v_3 + v_4, A_1$	3516.1280	95.1	10 6 a ₁	9 6 a ₂	$v_3 + v_4, A_1$	3551.3921	91.0
8 6 a ₂	7 3 a ₁	$v_3 + v_4, A_1$	3516.1495	96.1	10 6 a ₂	9 6 a ₁	$v_3 + v_4, A_1$	3551.4537	92.3
8 6 e	7 5 e	$v_3 + v_4, E$	3516.1959	57.8	11 3 a ₂	10 0 a ₁	$v_3 + v_4, A_1$	3551.5578	96.5
10 1 a ₂	9 3 a ₁	$v_1 + v_4, E$	3516.2771	91.1	10 7 e	9 7 e	$v_3 + v_4, A_1$	3554.4169	94.3
8 5 e	7 2 e	$v_3 + v_4, A_1$	3516.5863	96.1	11 3 a ₁	10 3 a ₂	$v_3 + v_4, A_1$	3554.8230	91.8
8 7 a	7 6 a	$v_3 + v_4, E$	3516.8843	38.8	11 3 a ₂	10 3 a ₁	$v_3 + v_4, A_1$	3556.2065	91.9
8 4 e	7 1 e	$v_3 + v_4, A_1$	3517.0611	93.7	12 12 e	11 11 e	$v_3 + v_4, E$	3557.7851	69.5
8 8 e	7 7 e	$v_3 + v_4, E$	3517.4233	40.2	12 8 e	11 7 e	$v_3 + v_4, E$	3557.9278	90.5
7 5 e	6 5 e	$v_3 + v_4, A_1$	3517.5380	82.8	12 9 e	11 8 e	$v_3 + v_4, E$	3558.2080	91.3
10 0 e	9 1 e	$v_1 + v_4, E$	3517.5728	79.4	12 11 e	11 10 e	$v_3 + v_4, E$	3558.2381	74.8
8 0 a ₁	7 0 a ₂	$v_3 + v_4, A_1$	3517.6297	84.7	12 10 a ₂	11 9 a ₁	$v_3 + v_4, E$	3558.4687	79.5
10 1 a ₁	9 0 a ₂	$v_3 + v_4, E$	3517.6817	75.6	12 10 a ₁	11 9 a ₂	$v_3 + v_4, E$	3558.4772	79.1
10 1 e	9 2 e	$v_3 + v_4, A_2$	3517.8793	93.2	11 6 a ₂	10 6 a ₁	$v_3 + v_4, A_1$	3562.4148	95.1
10 4 a ₁	9 6 a ₂	$v_1 + v_4, E$	3518.0770	98.4	11 6 a ₁	10 6 a ₂	$v_3 + v_4, A_1$	3562.5213	94.7
8 2 e	7 1 e	$v_3 + v_4, A_1$	3519.0751	89.7	13 13 a	12 12 a	$v_3 + v_4, E$	3567.5067	58.5
8 3 a ₁	7 0 a ₂	$v_3 + v_4, A_1$	3519.0940	87.7	13 12 e	12 11 e	$v_3 + v_4, E$	3568.2198	80.9
10 0 e	9 2 e	$v_1 + v_4, E$	3519.1293	97.1	13 10 a ₁	12 9 a ₂	$v_3 + v_4, E$	3568.6774	87.8
8 1 e	7 1 e	$v_3 + v_4, A_1$	3519.4776	87.4	13 10 a ₂	12 9 a ₁	$v_3 + v_4, E$	3568.6991	87.6
7 6 a ₂	6 6 a ₁	$v_3 + v_4, A_1$	3520.3165	91.7	13 11 e	12 10 e	$v_3 + v_4, E$	3568.7088	90.3
7 6 a ₁	6 6 a ₂	$v_3 + v_4, A_1$	3520.3278	91.2	14 13 a	13 12 a	$v_3 + v_4, E$	3578.0483	74.0
8 2 e	7 2 e	$v_3 + v_4, A_1$	3520.6493	86.4	14 12 e	13 11 e	$v_3 + v_4, E$	3578.6418	89.9

4. Estimation of vibrational parameters

For an analysis of high-resolution vibrational–rotational spectra of the bands which are located in higher wavelength regions, at least, approximate information about corresponding band centers can be very important. In this respect, it is useful to have information about harmonic frequencies ω_λ and anharmonic coefficients $x_{\lambda\mu}$ of a molecule. As to the PH_3 , such information, in principle, can be found in Ref. [3] where an ab initio quartic force field was derived. It should be mentioned, however, that the assumption about local mode behavior of the PH_3 molecule was additionally used in [3]. From this point, it would be interesting to compare the results of such ab initio calculations with the results of direct determination of vibrational spectroscopic parameters from experimental data.

At the moment, “experimental” values of vibrational energies are known for 12 vibrational states: the v_2 and v_4 bands were considered in [1]; the v_1 , v_3 , $2v_2$, $2v_4(A_1)$, $2v_4(E)$, and $v_2 + v_4$ were analyzed in Refs. [2,4]; information about the $v_1 + v_4$, $v_3 + v_4(E)$, $v_3 + v_4(A_1)$, and $v_3 + v_4(A_2)$ bands is presented in the present contribution. A simple calculation which can be made on this base lead to the results presented in Column 2 of Table 2. In that table, ω_λ , $x_{\lambda\mu}$, and g_{44} correspond to the usual notations used in vibrational–rotational spectroscopy [5]; g is the value of the E/A_λ vibrational splitting of the states $(0011, E)$ and $(0011, A_\lambda)$ ($\lambda = 1, 2$); d is the absolute values of shifts of the $(0011, E)$ and $(1001, E)$ terms caused by Fermi-type resonance interaction, see Fig. 4. For comparison, Column 3 of Table 2 presents the values of corresponding parameters obtained on the basis of ab initio calculations from [3]. Good correlations between the data in both Columns 2 and 3 can be seen for the first four parameters. It is not an unexcepted result because practically the same experimental data were used for corrections of ab initio calculations in [3].

The correspondence between the data in Columns 2 and 3 of Table 2 is worse for the other parameters presented. In this case, it is interesting to analyze situation with the three last combinations of parameters in Column 2. Firstly, let us use the x_{14} and x_{34} parameters from [3] in the last two

Table 2
Some vibrational spectroscopic parameters of the PH_3 molecule^a

Parameters	Our	From Ref. [3]
1	2	3
x_{22}	−5.85	−5.46
x_{24}	−2.29	−2.78
x_{44}	−2.87	−3.59
g_{44}	2.03	1.97
$\omega_2 + \frac{1}{2}x_{12} + x_{23}$	1006.11	1009.49
$\omega_4 + \frac{1}{2}x_{14} + x_{34}$	1126.04	1116.25
$2g - d$	5.04	—
$x_{14} - d$	−14.94	−16.07 ^b
$x_{34} + d$	−7.44	−17.87 ^b

^aAll the values are given in cm^{-1} .

^bHere x_{14} and x_{34} from [3] are given.

lines of Table 2. In this case, it is possible to determine two values of the d parameter, and they are 20.85 and -1.13 cm^{-1} , respectively. Comparison of these two values with each other allows one to come to the conclusion that the ab initio values of the parameters x_{14} and x_{34} do not satisfy the real experimental data. On the other hand, if one assumes the Fermi interaction is absent between the states $(0011, E)$ and $(1001, E)$, (i.e., $d = 0$ in Column 2), then results for the x_{14} and x_{34} parameters are $x_{34} = -7.44\text{ cm}^{-1}$, and $x_{14} = -14.94\text{ cm}^{-1}$, respectively. This result strongly differs from the values of corresponding parameters of [3], see Column 3.

It is well known in molecular spectroscopy that the anharmonic coefficients $x_{\lambda\mu}$ are negative, as a rule. As a consequence, data from Column 2 of Table 2 lead to the following condition for the d parameter, $-7.44 < d < 14.94\text{ cm}^{-1}$. At the same time, it should be mentioned that many manifestations of the local mode behavior can be seen in the vibration–rotation spectra of both the PH_3 molecule, and its deuterated species [5,6]. For this reason, one can assume that real values of the x_{14} and x_{34} parameters have to be close to each other. Under this assumption, one will obtain $x_{14} = x_{34} = -9.94\text{ cm}^{-1}$, $g = 5.02\text{ cm}^{-1}$, and $d = 5.00\text{ cm}^{-1}$. As the result of the discussion, we believe that these last values of parameters are not far from reality.

5. Conclusion

The high-resolution (0.005 cm^{-1}) Fourier transform infrared spectrum of PH_3 molecule was recorded for the first time in the region between 3280 and 3580 cm^{-1} , and assignments of the recorded transitions were fulfilled. In this case, because of strong resonance interactions between all the vibrational states of the studied poliad, transitions were assigned not only to the allowed bands $v_1 + v_4(E)$, $v_3 + v_4(E)$, and $v_3 + v_4(A_1)$, but also to the band $v_3 + v_4(A_2)$ which is forbidden on symmetry. Numerous a_1/a_2 splittings for the states $(J|K a_1, a_2)$ with the value of quantum number $K = 1\text{--}10$ were found in the experimental spectrum. Some pure vibrational spectroscopic parameters of the PH_3 molecule are estimated on the basis of analysis of experimental data.

Acknowledgements

This work was jointly supported by the National Project for the Development of Key Fundamental Sciences in China, by the National Natural Science Foundation of China (Grant Nos. 20103007 and 29903010), by the Foundation of the Chinese Academy of Science, and by the Ministry of Education of Russian Federation. O. Ulenikov and E Bekhtereva thank University of Science and Technology of China for guest professorship in 2002 year.

References

- [1] Ainetschian A, Häring U, Spiegl G, Kreiner WA. The v_2/v_4 Diad of PH_3 . J Mol Spectrosc 1996;181:99–107.
- [2] Ulenikov ON, Bekhtereva ES, Kozinskaia VA, Jing-Jing Zheng, Sheng-Gui He, Shui-Ming Hu, Qing-Shi Zhu, Leroy C, Pluchart L. On the study of resonance interactions and splittings in the PH_3 molecule: v_1 , v_3 , $v_2 + v_4$, and $2v_4$ bands. J Mol Spectrosc 2002;215:1–14.
- [3] Dong Wang, Qiang Shi, Qing-Shi Zhu. An ab initio quartic force field of PH_3 . J Chem Phys 2000;112:9624–31.

- [4] Tarrago G, Lacome N, Levy A, Guelachvili G, Bezard B, Drossart P. Phosphine spectrum at 4–5 μm : analysis and line-by-line simulation of $2\nu_2$, $\nu_2 + \nu_4$, $2\nu_4$, ν_1 , and ν_3 Bands. J Mol Spectrosc 1992;154:30–42.
- [5] Ulenikov ON, Petrunina OL, Bekhtereva ES, Sinitzin EA, Bürger H, Jerzembeck W. High resolution infrared study of PHD₂: The P–H stretching bands ν_1 and $2\nu_1$. J Mol Spectrosc 2002;215:85–92.
- [6] Ulenikov ON, Bekhtereva ES, Petrunina OL, Bürger H, Jerzembeck W. High resolution study of the ν_1/ν_5 and $2\nu_1/\nu_1 + \nu_5$ P–H stretching bands of PH₂D. J Mol Spectrosc 2003;218.